

On the electrooxidation of kraft black liquor on boron-doped diamond

Oliveira, Raisa C.P.; Buijnsters, Josephus G.; Mateus, Maria M.; Bordado, João C.M.; Santos, Diogo M.F.

DOI

[10.1016/j.jelechem.2022.116151](https://doi.org/10.1016/j.jelechem.2022.116151)

Publication date

2022

Document Version

Final published version

Published in

Journal of Electroanalytical Chemistry

Citation (APA)

Oliveira, R. C. P., Buijnsters, J. G., Mateus, M. M., Bordado, J. C. M., & Santos, D. M. F. (2022). On the electrooxidation of kraft black liquor on boron-doped diamond. *Journal of Electroanalytical Chemistry*, 909, Article 116151. <https://doi.org/10.1016/j.jelechem.2022.116151>

Important note

To cite this publication, please use the final published version (if applicable). Please check the document version above.

Copyright

Other than for strictly personal use, it is not permitted to download, forward or distribute the text or part of it, without the consent of the author(s) and/or copyright holder(s), unless the work is under an open content license such as Creative Commons.

Takedown policy

Please contact us and provide details if you believe this document breaches copyrights. We will remove access to the work immediately and investigate your claim.



On the electrooxidation of kraft black liquor on boron-doped diamond

Raisa C.P. Oliveira^{a,b}, Josephus G. Buijnsters^c, Maria M. Mateus^b, João C.M. Bordado^b,
Diogo M.F. Santos^{a,*}



^a Center of Physics and Engineering of Advanced Materials, Laboratory for Physics of Materials and Emerging Technologies, Chemical Engineering Department, Instituto Superior Técnico, Universidade de Lisboa, 1049-001 Lisbon, Portugal

^b Center for Natural Resources and the Environment, Chemical Engineering Department, Instituto Superior Técnico, Universidade de Lisboa, 1049-001 Lisbon, Portugal

^c Department of Precision and Microsystems Engineering, Faculty 3mE, Delft University of Technology, Mekelweg 2, 2628 CD Delft, The Netherlands

ARTICLE INFO

Keywords:

Kraft black liquor
Lignin
Electrooxidation
Boron-doped diamond

ABSTRACT

Black liquor (BL) is a highly alkaline byproduct from pulp mills. BL is rich in inorganic and organic compounds, with lignin (a natural polymer) being the most abundant. Following a waste biorefinery concept, the electrolysis of BL comprises lignin oxidation at the anode and hydrogen evolution at the cathode. These paired electrochemical processes show the promise to be carried out at lower cell voltage than that used in conventional alkaline water electrolyzers. Presently, new materials are required to improve the kinetics of the anodic reaction in the BL electrolyzer. Boron-doped diamond (BDD) can oxidize organic compounds at low overpotentials, making it a potential electrode material for BL oxidation. Herein, a BDD/Si electrode was produced, characterized by Raman spectroscopy and SEM, and employed for the oxidation of BL. The properties of the used kraft BL were determined, namely the pH (12.7), conductivity (470 mS cm^{-1}), organic/inorganic ratio (1.0), and Klason lignin content (42.2 g L^{-1}). Fourier-transform infrared spectroscopy was also used in the BL characterization. The BDD performance for BL oxidation was assessed by cyclic voltammetry, chronopotentiometry, and chronoamperometry. A number of exchanged electrons and a charge transfer coefficient of 3.0 and 0.8, respectively, were calculated. It was demonstrated that BDD presents a good activity for BL oxidation, comparable to that of platinum.

1. Introduction

Diamond is a crystalline allotrope of carbon and possesses the highest hardness of any natural material, high chemical resistance, and high thermal conductivity. Diamond is very popular in the jewelry industry due to its unique properties, making it a valuable material. Natural diamond presents high electrical resistivity, which prevents its use as an electrode [1,2]. However, if the diamond is intentionally doped with boron, it becomes conductive due to the introduction of impurity levels in the band gap (substitutional boron has an acceptor level of 0.37 eV above the valence band maximum). For boron concentrations up to $\sim 2 \times 10^{20} \text{ cm}^{-3}$, the B-doped material shows p-type semiconductor behavior [1,3], and metallic conductivity is found for heavily doped diamond ($> 2 \times 10^{20} \text{ cm}^{-3}$). Boron-doped diamond (BDD) thin films can be synthesized on a wide variety of substrates by using chemical vapor deposition methods. Thus produced polycrystalline BDD electrodes have received considerable attention in the last decades [2,4] due to their promising performance in the environmental area [2,5].

BDD has been widely used in the direct or indirect oxidation of compounds (especially the organic ones) due to its high potential for the oxygen evolution reaction (OER) (above 2.2 V vs. SHE). In other words, it means that BDD has a wide potential window where it can be active as an anode without being affected by the OER side reaction [2,6]. Due to this unique feature, BDD has been applied as an electrode for the treatment of wastewaters to decrease the amount of organic pollutants by a direct or an indirect process. In the case of direct oxidation, the electrons flow from the contaminant to the positive electrode, i.e., the anode, at potentials above a specific value. Generally, a wide variety of substances can be formed through direct oxidation (e.g., carboxylic acid derivatives, CO_2) depending on the target contaminant, operating conditions, or electrolyte composition [5,7,8]. In most cases, the easily oxidized portions are removed through direct oxidation, leading to a more persistent molecular structure.

On the other hand, indirect oxidation leads to simultaneous electro-generation of different active species (depending on the ion availability), including oxidant species (e.g., H_2O_2 , O_3 , active chlorine, $\text{SO}_4^{\bullet-}$, $\text{CO}_3^{\bullet-}$) able to promote the mineralization of organic compounds. In

* Corresponding author.

E-mail address: diogosantos@tecnico.ulisboa.pt (D.M.F. Santos).

the case of the indirect oxidation *via* OER, the process is based on the existence of OH^\bullet radicals [5,9–12]. Indirect oxidation demands more energy than direct oxidation since the overpotential for reaching OER and, consequently, radicals' production is relatively high. However, it is useful for reactions in which the BDD surface may undergo severe changes [1], such as electrode fouling [5].

BDD also presents other features that contribute to an excellent electrochemical performance in environmental electrochemistry, including (i) an inert surface with low adsorption capacity (increasing its resistance to poisoning and deactivation) [7,13], (ii) chemical stability and corrosion resistance, due to the strong carbon–carbon covalent bond in the diamond and the resistant hybrid sp^3 orbitals [6,9], and (iii) possible manipulation of its composition, surface morphology, and conductivity, namely by changing the dopant concentration, the substrate, and/or synthesis method, thus improving BDD activity for a particular reaction [14,15]. Because of the above-mentioned properties, BDD has been successfully used for the oxidation of phenolic compounds [12,16–18], pharmaceutical compounds [10,19,20], dyes [21], and wastewaters [5,22–24], just to name a few.

Considering the outstanding capacity for incineration/oxidation of organic compounds, BDD has been recently reported as a suitable electrode for the treatment of woodworking and paper wastewater, leading to COD removals of 93% (at 45 mA cm^{-2} for 200 min) and 85% (at $10\text{--}30 \text{ mA cm}^{-2}$ for 180 min), respectively [23,25]. The present study assessed the activity of BDD for the oxidation of black liquor (BL), a byproduct from pulp and paper mills. BL presents similarities with woodworking wastewater since it contains similar organics (lignin, cellulose, hemicellulose, and sugars) [23,26–29]. BL is usually recycled for chemical recovery and energy generation, but a BL excess can be generated during production peaks. This excess of BL should be treated or consumed by a simple and economical process, avoiding costly treatments for its safe disposal. Many works have been focused on finding a final destination for the BL. The proposed strategies include acid-precipitation, membrane-assisted, and biodegradation (employing different bacteria) techniques [30–37], as well as electrochemistry-related approaches [29,38–48]. However, to the best of our knowledge, BDD was not tested as an electrode for BL oxidation until now.

Thus, this work aimed to analyze the potential of BDD as an electrode for the oxidation of *Eucalyptus globulus* BL from a kraft pulp mill. Despite the complex nature of kraft BL composition, it has high ionic conductivity due to the cooking chemicals (NaOH , Na_2S , Na_2CO_3), making the addition of a supporting electrolyte unnecessary. BL also contains a high concentration of lignin fractions formed during the cooking process. When the fibers separate, lignin is broken into shorter length fractions ($M_w < 2000 \text{ g mol}^{-1}$) that are easier to solubilize. These features make BL an adequate electrolyte solution to perform lignin electrooxidation [29,38,49,50].

The electrooxidation of lignin occurs at lower potentials than the OER [50,51]. This means that in a BL electrolyzer, the hydrogen evolution reaction (HER) occurs at the cathode side, while lignin oxidation takes place at the anode side. The latter reaction does not generate gaseous products but low-molecular-weight compounds, such as heptane, phenol, apocynin, and vanillin [40,48,49,52,53]. Thus, membrane separators are unnecessary for BL electrolyzers, as pure hydrogen (H_2) is the only gas generated. Additionally, the required cell voltage should be lower than that employed in a typical alkaline water electrolyzer for H_2 production [38,41,42]. These two factors lead to a lower cost of the BL electrolyzer.

The H_2 produced at the cathode of the proposed BL electrolyzer is currently seen as a sustainable energy carrier. It may be used to generate electricity in a fuel cell (e.g., to power a forklift), blend in the natural gas network, or even increase the temperature in the recovery furnace (where the inorganic salts of the cooking process are recovered). On the other hand, the valuable low-molecular-weight compounds generated at the anode can be recovered following the biorefinery concept, thus increasing the economic value of the BL.

Thus, considering the excellent activity of BDD for the oxidation of organic compounds at low potentials, this material seems to possess all the features needed to be a high-performance electrode for the oxidation of the lignin contained in BL [2,54]. If the electrochemical studies confirm this hypothesis, the BDD anode can decrease the ΔE needed for a cost-effective BL electrolyzer operation. Herein prepared BDD was grown by hot-filament chemical vapor deposition (CVD) technique and characterized by scanning electron microscopy (SEM) and Raman spectroscopy. The BL sample was physicochemically characterized, and parameters such as ash, lignin, and dry solids content were determined. Fundamental electrochemical studies, including cyclic voltammetry (CV), chronopotentiometry (CP), and chronoamperometry (CA), were done at 25°C employing BL as the electrolyte. The electrocatalytic activity of BDD was assessed, and the kinetic parameters were determined.

2. Experimental

2.1. Synthesis of the BDD/Si electrode

Hot-filament CVD was used to grow a $4\text{-}\mu\text{m}$ thick polycrystalline and heavily doped BDD film on a silicon wafer, following a seeding procedure described elsewhere [55]. BDD film growth was achieved at a substrate temperature of about 850°C using three-gas chemistry of tri-methylborane/methane/hydrogen ($40 \text{ sccm}/72 \text{ sccm}/3000 \text{ sccm}$) at 8 mbar atmosphere [56]. The achieved B-doping level was $\sim 2.8 \text{ at.}\%$, and the BDD film resistivity was $\sim 5 \times 10^{-3} \Omega \text{ cm}$ [57]. Identical BDD/Si electrodes were produced by dicing the grown wafer into adjacent square pieces of about $15 \times 15 \text{ mm}^2$.

2.2. Characterization of the BDD/Si electrode

SEM analysis of the electrode surface was done in secondary electron imaging mode using a JEOL JSM-6010LA scanning electron microscope with an acceleration voltage of 15 kV. Atomic force microscopy (AFM) measurements were done in dynamic mode to analyze the surface topography. AFM scans were performed using a NaniteAFM (Nanosurf) with areas of $15 \times 15 \mu\text{m}^2$, and post-processing was done using Gwyddion v2.57 software. Raman spectroscopy was done with a Horiba LabRAM HR setup, equipped with an argon-ion laser (excitation wavelength 514 nm) and a spectral resolution of $\sim 0.3 \text{ cm}^{-1}$.

2.3. Characterization of the black liquor sample

The kraft black liquor (BL) was provided by *The Navigator Company*, a Portuguese *Eucalyptus globulus* pulp mill (Cacia, Portugal). BL sample was characterized by Fourier-transform infrared spectroscopy (FTIR) employing a PerkinElmer Spectrum Two FTIR spectrometer coupled with an attenuated total reflection (ATR) accessory. The air was considered the blank, and all experiments were done in the range $500\text{--}4500 \text{ cm}^{-1}$ (10 scans with a resolution of 5 cm^{-1}). pH and conductivity of the BL were measured in a Hanna Instruments edge® Multiparameter HI2020 employing a HI11310 and a HI763100 probe, respectively. The BL total solids content (TSC, dry matter) was acquired by a VWR IT 1,400,108 moisture analyzer balance. Ash content was obtained according to the standard method for ash in biomass, ASTM E1755 – 01(2020) [58]. BL density (ρ) was experimentally determined with a pycnometer following ASTM D1217-15 standard procedure [29,59].

Klason (or acid-insoluble) lignin (KL) content in BL was determined in triplicate through the following steps: (i) removal of most of the water in a BUCHI Rotavapor™ R-300 Rotary Evaporator with Controller and V-300 Pump; (ii) drying at 60°C in a Memmert DIN 40050-IP20 oven during overnight; (iii) drying at 105°C for 2 h;

(iv) letting the samples cool down in a desiccator; (v) following the Klason lignin content procedure (based on T222 om-88 [60]).

2.4. Electrochemical measurements

Electrochemical measurements were carried out in a three-electrode electrochemical cell ($V = 50$ mL) employing a saturated calomel electrode (SCE) as a reference, a platinum coil counter-electrode, and BDD as the working electrode ($A = 0.071$ cm²). Recorded potentials were converted to the reversible hydrogen electrode (RHE) scale using the expression $E_{\text{RHE}} = E_{\text{SCE}} + 0.242 + 0.059 \times \text{pH}$. All potentials given in the manuscript refer to the RHE scale. A Squidstat Plus potentiostat/galvanostat from Admiral Instruments and the associated Squidstat User Interface software were used for total control of the experiments. BDD electrode was gently washed with Millipore water followed by preactivation in BL by running 20 consecutive CVs at 200 mV s⁻¹ in the -0.3 V – 0.6 V range to remove any impurity from the electrode surface. Cyclic voltammetry (CV) in a wide potential window (-0.3 – 2.0 V) was used to assess the BDD electrode activity in the BL and in a blank solution with the same pH of the BL (upon NaOH (0.05 M) addition). The composition of such blank solution was 0.05 M NaOH (pH = 12.7, same as in BL). Then, CVs were run at scan rates, ν , ranging from 5 to 500 mV s⁻¹ in the potential window between the open circuit potential (OCP, ca. 0.3 V) and 1.5 V. Chronoamperometry (CA) studies were done at potentials ranging from 0.3 to 1.3 V and chronopotentiometry (CP) measurements were run in the 1.4 – 31.8 mA cm⁻² range. All experiments were done at room temperature (ca. 25 °C) under diffusion-limited conditions.

3. Results and discussion

3.1. Characterization of the BDD/Si electrode

A top-view SEM image of the BDD/Si electrode surface is shown in Fig. 1A. The BDD film shows a highly faceted surface with a wedge-shaped (111) crystal orientation. The diamond crystallites vary in size from 0.3 to 1.8 μm (with average sizes around 1 μm), which results in AFM root-mean-square surface roughness of around 0.26 μm .

The Raman spectrum obtained from the BDD/Si electrode surface (Fig. 1B, where the intensity is normalized to 1.0 for the most intense peak) is typical for a heavily B-doped diamond film [57]. Two broad and intense peaks located at ~ 450 and ~ 1200 cm⁻¹ dominate the Raman spectrum. These signals, referred to as the lower and higher boron peaks, respectively, arise from the incorporation of high levels of boron dopants into the diamond lattice. Fano resonance leads to the strong distortion of the diamond one-phonon line (1332 cm⁻¹), which becomes barely visible. On the contrary, the G-band

(1530 cm⁻¹) is well visible, likely arising from graphitic material [61] present in the BDD film's grain boundaries.

3.2. Characterization of the black liquor sample

A conductivity of 470 mS cm⁻¹ and a pH of 12.7 were obtained for BL. The TSC was found to be 15.5%, determined from an initial and final mass of 9.76 g and 1.51 g, respectively. Those parameters agree with previous results reported in the literature for weak BL [26,29,34,38,62].

Most of the total lignin contained in BL (as well as in wood) is Klason lignin [63–65], the remaining acid-soluble lignin. The Klason lignin content in BL was 30.2 ± 0.7 wt% (on a dry basis), in agreement with previous reports [30,66]. It was assumed to match the total lignin concentration in BL ($C = 42.2$ g L⁻¹) since the acid-soluble lignin content is considerably lower than the Klason one [65,67]. A relative density, ρ , of 1097 kg m⁻³ was used to determine C.

The ash content was determined on a dry basis by dividing the mass recorded after the ash determination procedure, corresponding to the inorganic components in the BL solids, over the mass of BL dry solids at the beginning of the experiment. An average value of 49.6 ± 1.4 wt% was found for the ash content. This value corresponds to an organic/inorganic ratio of 1.0, in agreement with previous reports [29,38,42,68].

The FTIR spectrum of the BL is presented in Fig. 2 (the absorbance is normalized).

It exhibits well-defined peaks, mainly from lignin species, which are detailed and compared with the literature values in Table 1.

The FTIR spectrum shows most organic and inorganic groups present in the BL composition. The aromatic, C=C, and C=O vibrations are mostly associated with the complex structure of the organic compounds. For example, the C=O bond valence vibration appearing at 1637 cm⁻¹ is usually associated with a *p*-substituted aryl ketone of lignin's guaiacyl group [76]. The peak assigned at 1120 cm⁻¹ (inset of Fig. 2 is one of the most used for identifying lignin in samples, since it is susceptible to oscillations in the concentration of this natural polymer [75].

The BL's inorganic compounds are also active in infrared. The S=O band at 620 cm⁻¹ is related to SO₄²⁻ ion, coming from the sodium and potassium sulfate salts added during the wood (kraft) cooking process [70,77]; the signal at 1412 cm⁻¹ is associated with the carbonate ion [71].

3.3. Electrochemical studies

The behavior of BDD was first analyzed in a blank solution with the same pH of the BL (pH = 12.7, equivalent to 0.05 M NaOH) to assure

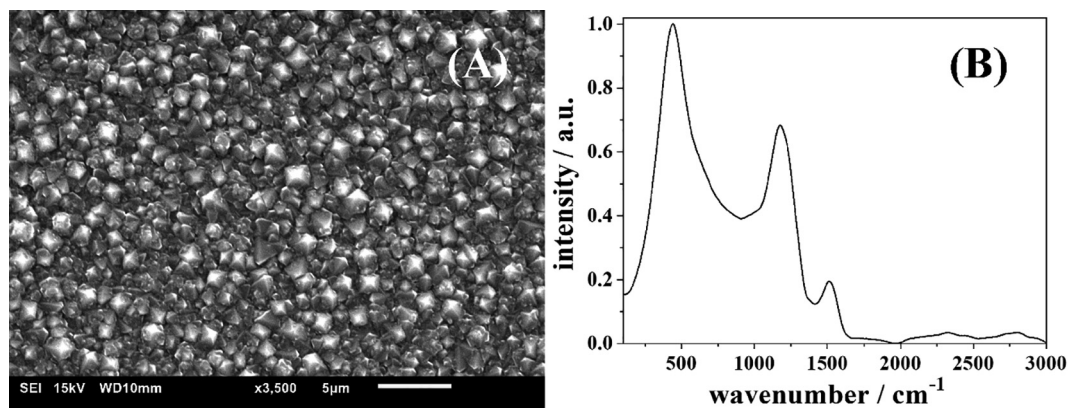


Fig. 1. (A) SEM image (top-view) and (B) Raman spectrum of the BDD/Si electrode.

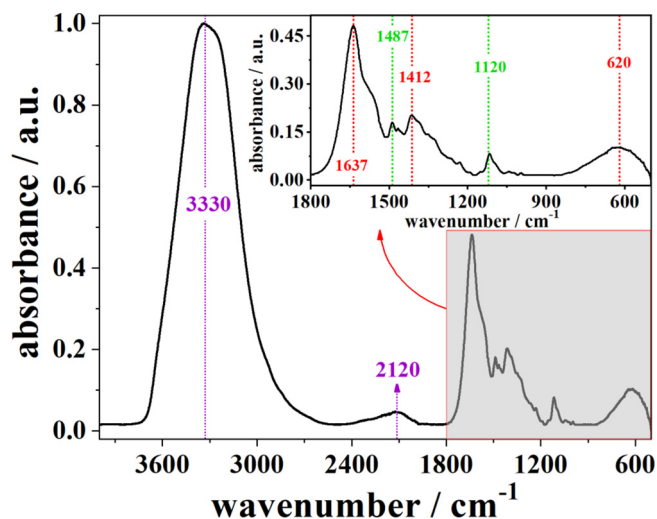


Fig. 2. FTIR spectrum of the BL. Inset shows a zoom of the 500–1800 cm^{-1} region.

Table 1

Peak assignment in the FTIR spectrum of the BL.

Experimental band / cm^{-1}	Vibration	Reference band / cm^{-1}
3330	OH stretching – intramolecular hydrogen bonding in an aqueous solution [69]	3300 [69]
2120	Asymmetrical C=C stretching (the symmetric one is FTIR inactive) [70,71]	2125 [70,71]
1637	C=O stretching (non-conjugated ketones, carbonyl, and ester groups) [72]	1640–1600 [69] 1635 [72]
1560	Antisymmetric stretching vibration of CO_2^- [69,73]	1695–1540 [69] 1550 [73]
1487	Aromatic ring semi-circle stretching [70], usually with origin in guaiacyl group of lignin [73]	1525–1470 [70] 1491 [73]
1412	Symmetric CO_2^- stretch [69,73]	1440–1355 [69] 1405 [73]
1120	Aromatic skeletal and C–O stretching [74]	1122 [74] 1123 [75]
620	S=O stretching vibration [70]	620 [70]

the BDD electrochemical inertia in the working potential window. As shown in Fig. 3A, BDD does not exhibit any redox processes in the blank solution (0.05 M NaOH). In the BL, a single anodic peak at ca. 1.1 V is detected in the 1st cycle, whereas two well-defined anodic peaks, at ca. 0.8 V and 1.1 V, are observed for the 2nd, 3rd, and 4th cycles (Fig. 3A, with the CVs practically overlapping after the first cycle). This establishes BDD as an active electrode material for the oxidation of BL, which is directly associated with its activity for lignin oxidation [29,38,42,78]. No peak is noted in the back scan of the CV in BL, typical for organic compounds where their oxidation product is converted to a non-electrochemically active compound. This may occur either by decomposition or by direct reaction with the solvent or any other compound present in the electrolyte solution [79], known as an electrochemical–chemical (EC) mechanism [79,80]. The different shape and higher current density of the anodic peak in the 1st cycle suggest possible film formation at the BDD electrode surface [38]. This does not affect the stability of the electrode activity, as all subsequent CVs show an overlap (Fig. 3A).

For potentials above ca. 1.6 V, the recorded currents are significantly higher in BL than in the 0.05 M NaOH blank solution, suggesting enhancement of the OER. This owes to the higher ionic conductivity of the BL when compared to the blank solution. Contrary to the blank solution, containing only 0.2 wt% NaOH, BL contains many other inorganic compounds, such as Na_2S , Na_2CO_3 , and Na_2SO_4 , with concentrations around 0.6, 2.1, and 3.2 wt%, respectively.

Fig. 3B shows the effect of the scan rate in the BL CVs in the 5 – 500 mV s^{-1} range. At low scan rates (5, 10, and 20 mV s^{-1}), the anodic peak (p_1) at ca. 0.8 V is associated with a first oxidation process occurring at lower overpotentials. A well-defined second peak, p_2 , appears in the 1.0 – 1.3 V potential range in the CVs obtained at all scan rates. Similar BL voltammogram shapes were observed employing platinum (Pt), nickel (Ni), and stainless steel (SS) electrodes [38,42,78]. The longer the scan lasts, the thicker is the diffusion layer, and, consequently, the reaction is more controlled by mass transfer [81]. With the increase of scan rate, the p_1 shape becomes ill-defined, suggesting that the process is controlled by charge transfer (kinetic control) [82]. On the other hand, the second peak, p_2 , shows a diffusion-controlled behavior since it is sharper for higher scan rates [82,83]. An increase of the current density with the increase of the scan rate is observed for both p_1 and p_2 . Additionally, p_2 potential shifts to the right for higher scan rates, i.e., higher peak potential, E_{p_2} , values, a behavior usually associated with irreversible electrochemical processes [82,83], while p_1 maintains its E_{p_1} values almost constant. The absence of a peak in the back scan suggests that both reactions occurring at p_1 and p_2 are irreversible. However, only p_2 pre-

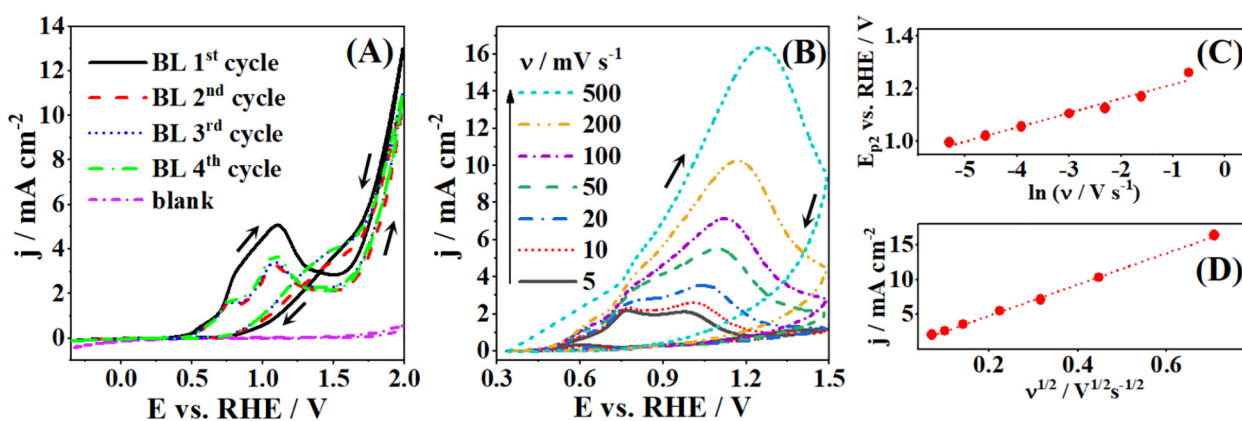


Fig. 3. (A) CVs at 50 mV s^{-1} of the BDD electrode in BL (4 consecutive cycles) and in blank solution (0.05 M NaOH) with the same pH. (B) Effect of the scan rate on the CVs of BDD in BL, with the corresponding (C) E_{p_2} vs. $\ln v$ and (D) j_{p_2} vs. $v^{1/2}$ regressions for the second peak, p_2 . All experiments were done at 25 °C in the absence of convection.

sents a behavior adequate for the application of Eq. (1), being shifted to more positive potentials with increasing ν [38,82,83],

$$E_p = E^0 + \left[\frac{RT}{(1-\alpha)n_a F} \right] \left\{ 0.78 + \ln \frac{D}{k_s} + \ln \left[\frac{(1-\alpha)n_a F \nu}{RT} \right]^{1/2} \right\} \quad (1)$$

where E_p is the peak potential, R is the universal gas constant ($8.314 \text{ J K}^{-1} \text{ mol}^{-1}$), E^0 is the formal potential, α is the charge transfer coefficient, T is the temperature (K), n_a is the number of electrons involved in the rate-determining step (considered as 1), F is the Faraday constant (96485 C mol^{-1}), D is the lignin diffusion coefficient in the BL, k_s is the standard heterogeneous rate constant (cm s^{-1}), and ν is the scan rate (V s^{-1}). Stokes-Einstein equation was used to calculate a D value of $1.203 \times 10^{-6} \text{ cm}^2 \text{ s}^{-1}$, considering an average lignin molecular weight of 870 g mol^{-1} [84,85]. Lignin is assumed to be the organic compound oxidized during both p_1 and p_2 processes [29,38,86]. An E_{p2} vs. $\ln \nu$ regression was drawn (Fig. 3C) and an α_{p2} of 0.8 was calculated from its slope.

The number of exchanged electrons at p_2 was calculated considering the α_{p2} value previously obtained from the j_{p2} vs. $\nu^{1/2}$ regression (Fig. 3D) by applying the Randles-Sevcik equation for irreversible systems valid for $T = 298 \text{ K}$ (Eq. (2)),

$$j_p = 2.99 \times 10^5 [(1-\alpha)n_a]^{1/2} n C (D\nu)^{1/2} \quad (2)$$

where j_p is the peak current density in mA cm^{-2} , n is the number of exchanged electrons per lignin molecule, and C is the lignin concentration in mol cm^{-3} . A value of $n_{p2} = 2.3$ was determined.

Table 2 summarizes the recorded OCP values, BL oxidation onset overpotentials, η_0 , charge transfer coefficients, α , and the number of exchanged electrons, n , obtained for the oxidation of *Eucalyptus* BL at Pt, Ni, SS, and BDD electrodes at 25°C .

η_0 consists of the difference between OCP and the onset potential for BL oxidation. A large η_0 means extra energy required for the oxidation reaction in a real BL electrolyzer. On the other hand, the α value points which process is favored according to the variation of the free Gibbs energy [83], with an α of 0.5 indicating a reversible electrode process. Finally, higher n values mean higher faradaic efficiency and, consequently, higher currents for BL oxidation [81,82].

By analyzing the different materials tested (Table 2), the performance of the electrodes is ordered as $\text{BDD} = \text{Pt} > \text{Ni} \square \text{SS}$, where Pt and BDD perform the best and SS the worst. BDD shows an excellent activity for BL oxidation, presenting a high number of exchanged electrons ($n = 2.3$) and an α value ca. 30% larger than that of Pt. Also, the low η_0 value for BDD shows the excellent capacity of this material to oxidize the organic matter in the BL.

Chronopotentiometry (CP), a galvanostatic technique run in diffusion-limited conditions, was employed to verify the number of consecutive oxidations in the system by checking the number of 'plateaus' present in each chronopotentiogram [82]. Fig. 4A shows the CP curves for current densities in the $10.6 - 31.8 \text{ mA cm}^{-2}$ range. The curves have different durations because they are run for the time needed to determine the transition time, τ , of each oxidation reaction.

Two plateaus are observed for all recorded CPs (Fig. 4A). The first one, occurring in the $1.0 - 1.4 \text{ V}$ potential range, is related to the lignin oxidation at the BDD surface. In the absence of convection, the lignin in the vicinity of the electrode is quickly oxidized, and the potential rises to the following possible anodic process. This second plateau,

above 1.9 V , is not related to BL oxidation but to the oxygen evolution reaction (OER), since no other peak was noticed in the CV studies (Fig. 3A). A decrease of τ was noted with increasing j , as expected [29,82,83]. Considering the linear behavior observed in $\tau^{1/2}$ vs. j^{-1} (Fig. 4B) with an excellent correlation coefficient ($R^2 = 0.996$), it is possible to employ the Sand equation (Eq. (3)).

$$\tau^{1/2} = nFC(\pi D)^{1/2} (2j)^{-1} \quad (3)$$

From the slope of the Sand regression (Fig. 4B), an n value of 3.0 was calculated. This number is slightly higher than those obtained by CV ($n = 2.3$), which can be justified by the occurrence of both p_1 and p_2 processes simultaneously during the first plateau recorded in the CP experiments, leading to a number of exchanged electrons that corresponds to the sum of the n values for the two peaks.

Finally, chronoamperometry (CA) was used to determine the number of exchanged electrons at different applied potentials using the Cottrell equation (Eq. (4)).

$$j = nFD^{1/2} C \pi^{-1/2} t^{-1/2} \quad (4)$$

Fig. 5A presents a CA run at 1.1 V and the corresponding Cottrellian regression (j vs. $t^{-1/2}$), exhibiting an excellent fitting. The number of exchanged electrons obtained for the different applied potentials (ranging from 0.8 to 1.2 V) is shown in Fig. 5B.

The behavior observed in Fig. 5B has been previously reported [29]. There is a maximum around the potential of p_1 and a second maximum at a potential where is reported the presence of p_2 (Fig. 3A and B), corresponding to the highest number of exchanged electrons ($n \approx 2.0$) obtained for CA experiments.

The results obtained using these three electrochemical techniques suggest that BL oxidation at the BDD electrode occurs via two oxidation processes (p_1 and p_2). p_2 involves a higher n value, leading to a more extensive modification in the BL composition.

As discussed above, the relevant oxidation process in BL is lignin oxidation. This organic polymer is usually shorter in BL than in nature due to the pulping process to which the wood is subjected [87–89]. Thus, BL lignin is more susceptible to the electrochemical process, as it is shorter and has a negative charge, making it a potential electron donor [29,38,84,85].

The maximum value of exchanged electrons in BL lignin oxidation is unknown since BL contains lignin molecules with different lengths and molecular weights. However, recent fundamental studies on the topic are helping to understand which materials are more active for lignin electrooxidation. Pt, Ni, and BDD electrodes are the most effective reported so far [29,38].

4. Conclusions

This work deals with the development of electrode materials for the BL electrolyzer, a system that can simultaneously produce H_2 and low-molecular-weight organic compounds, following a waste biorefinery concept. It is known that BDD is a potential anode material for the oxidation of organic compounds, namely those present in wastewater, due to its high overpotential for HER and OER. Considering that, BDD was herein tested as an electrode for the oxidation of BL.

CV, CP, and CA techniques were employed to understand the electrochemical behavior of BL at the BDD electrode and to determine

Table 2
Summary of parameters obtained for *Eucalyptus globulus* BL oxidation at different electrodes.

Electrode	OCP vs. RHE / V	η_0 / mV	α	n	Source
BDD	0.3	200	0.8	2.3	This work
Pt	0.3	200	$0.5_{p1}/0.6_{p2}$	$1.2_{p1}/2.7_{p2}$	[38]
Ni	0.4	200	0.5	1.6	[38]
SS	0.3	700	0.9	2.4	[38]

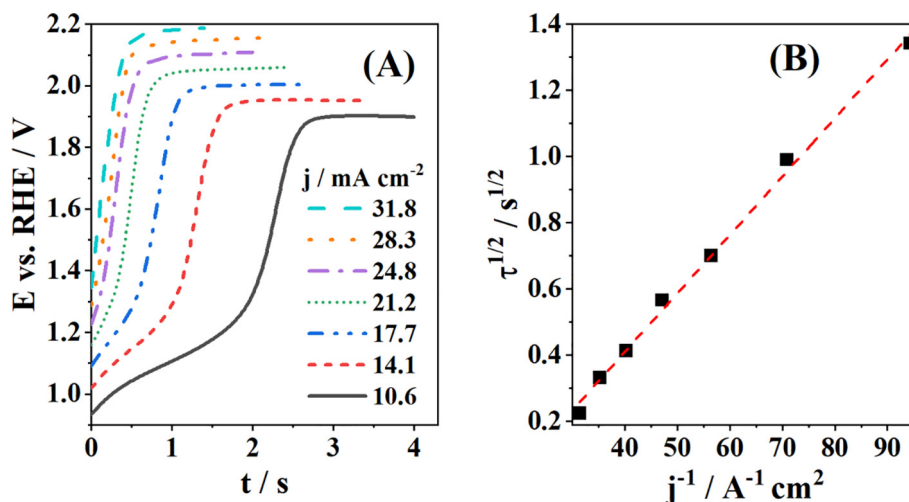


Fig. 4. (A) CPs obtained for BL oxidation at BDD electrode for different current densities and (B) the corresponding Cottrell regression. All experiments were done at 25 °C in the absence of convection.

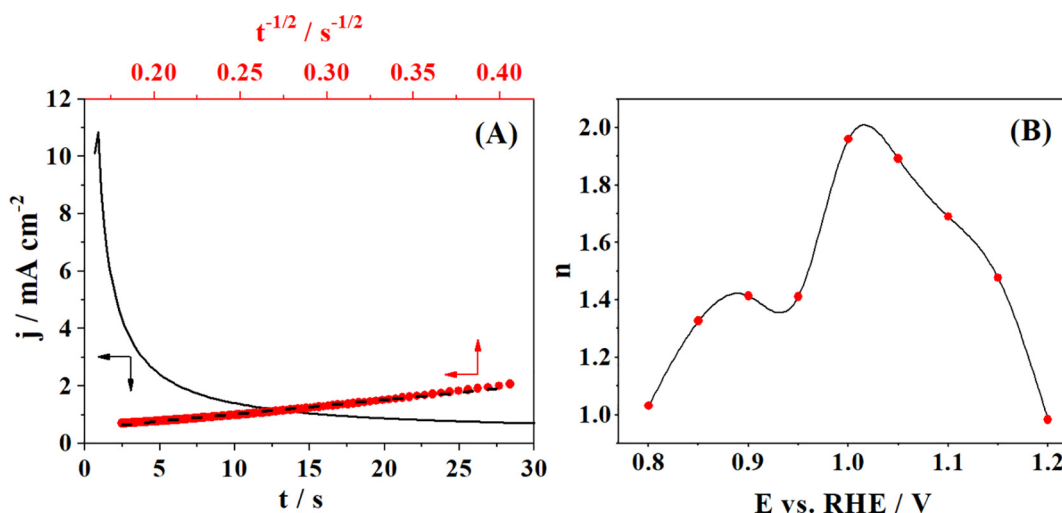


Fig. 5. (A) CA response (and the respective Cottrellian regression) at 1.1 V and (B) the effect of the applied potential on the number of exchanged electrons determined by CA. All experiments were done at 25 °C in the absence of convection.

kinetic parameters. It was possible to conclude that BL oxidation at the BDD electrode occurs via two irreversible processes. In the first one (p_1), the exchange of ~ 1 electron occurs, while in the second (p_2), 2 electrons are extracted from BL. A low onset overpotential of 200 mV was found for the oxidation process at BDD, similar to that obtained with a Pt electrode. This overpotential is significantly lower than those reported for OER [51]. Thus, a BL electrolyzer comprising a BDD anode has the potential to generate H_2 at lower cell voltages than typical alkaline electrolyzers. Also, the generated H_2 would have higher purity, as there is no generation of other gases at the anode, such as oxygen. This allows avoiding the use of expensive membrane separators, making the BL electrolyzer design simpler than conventional water electrolyzers. In addition, lignin oxidation products with added value can be recovered from the BL after electrolysis and subsequently commercialized.

CRediT authorship contribution statement

Raisa C.P. Oliveira: Investigation, Methodology, Writing – original draft. **Josephus G. Buijnsters:** Investigation, Writing – original draft. **Maria M. Mateus:** Data curation, Validation. **João C.M. Bor-**

dado: Visualization, Funding acquisition, Supervision. **Diogo M.F. Santos:** Conceptualization, Supervision, Writing – review & editing.

Declaration of Competing Interest

The authors declare that they have no known competing financial interests or personal relationships that could have appeared to influence the work reported in this paper.

Acknowledgments

The authors would like to thank Fundação para a Ciência e a Tecnologia (FCT, Portugal) for a research contract in the scope of programmatic funding UIDP/04540/2020 (D.M.F. Santos) and PhD grant SFRH/BD/137470/2018 (R.C.P. Oliveira), and the Dutch Research Council (NWO) for funding project no. 16361 through the Open Technology Programme (J.G. Buijnsters). Prof. Wilfried Vanderhorst (imec, KU Leuven) and Dr. André F. Sartori (Delft University of Technology) are acknowledged for their help with the supply and preparation of the BDD electrode, respectively. *The Navigator Company* is gratefully acknowledged for providing the black liquor samples.

References

- [1] J.H.T. Luong, K.B. Male, J.D. Glennon, Boron-doped diamond electrode: Synthesis, characterization, functionalization and analytical applications, *Analyst* 134 (2009) 1965–1979, <https://doi.org/10.1039/b910206j>.
- [2] P.V. Nidheesh, G. Divyapriya, N. Oturan, C. Trellu, M.A. Oturan, Environmental applications of boron-doped diamond electrodes: 1, Applications in water and wastewater treatment, *ChemElectroChem* 6 (2019) 2124–2142, <https://doi.org/10.1002/celec.201801876>.
- [3] S. Lips, S.R. Waldvogel, Use of boron-doped diamond electrodes in electro-organic synthesis, *ChemElectroChem* 6 (6) (2019) 1649–1660, <https://doi.org/10.1002/celec.v6.610.1002/celec.201801620>.
- [4] N. Vinokur, B. Miller, Y. Avyigal, R. Kalish, Electrochemical behavior of boron-doped diamond electrodes, *J. Electrochem. Soc.* 143 (1996) L238–L240, <https://doi.org/10.1149/1.1837157>.
- [5] Y. He, H. Lin, Z. Guo, W. Zhang, H. Li, W. Huang, Recent developments and advances in boron-doped diamond electrodes for electrochemical oxidation of organic pollutants, *Sep. Purif. Technol.* 212 (2019) 802–821, <https://doi.org/10.1016/j.seppur.2018.11.056>.
- [6] H.B. Suffredini, S.A.S. Machado, L.A. Avaca, The water decomposition reactions on boron-doped diamond electrodes, *J. Braz. Chem. Soc.* 15 (2004) 16–21, <https://doi.org/10.1590/S0103-50532004000100004>.
- [7] M. Panizza, G. Cerisola, Direct and mediated anodic oxidation of organic pollutants, *Chem. Rev.* 109 (12) (2009) 6541–6569, <https://doi.org/10.1021/cr9001319>.
- [8] J.-F. Zhi, H.-B. Wang, T. Nakashima, T.N. Rao, A. Fujishima, Electrochemical incineration of organic pollutants on boron-doped diamond electrode. Evidence for direct electrochemical oxidation pathway, *J. Phys. Chem. B* 107 107 (48) (2003) 13389–13395, <https://doi.org/10.1021/jp030279g>.
- [9] T.A. Enache, A.-M. Chiorcea-Paquim, O. Fatibello-Filho, A.M. Oliveira-Brett, Hydroxyl radicals electrochemically generated in situ on a boron-doped diamond electrode, *Electrochem. Commun.* 11 (7) (2009) 1342–1345, <https://doi.org/10.1016/j.elecom.2009.04.017>.
- [10] M. Panizza, A. Dirany, I. Sirés, M. Haidar, N. Oturan, M.A. Oturan, Complete mineralization of the antibiotic amoxicillin by electro-Fenton with a BDD anode, *J. Appl. Electrochem.* 44 (12) (2014) 1327–1335, <https://doi.org/10.1007/s10800-014-0740-9>.
- [11] S.O. Ganiyu, M. Gamal El-Din, Insight into in-situ radical and non-radical oxidative degradation of organic compounds in complex real matrix during electrooxidation with boron doped diamond electrode: A case study of oil sands process water treatment, *Appl. Catal. B Environ.* 279 (2020) 119366–119374, <https://doi.org/10.1016/j.apcatb.2020.119366>.
- [12] Y.U. Shin, H.Y. Yoo, Y.Y. Ahn, M.S. Kim, K. Lee, S. Yu, C. Lee, K. Cho, H. il Kim, J. Lee, Electrochemical oxidation of organics in sulfate solutions on boron-doped diamond electrode: Multiple pathways for sulfate radical generation, *Appl. Catal. B Environ.* 254 (2019) 156–165, <https://doi.org/10.1016/j.apcatb.2019.04.060>.
- [13] V. Suryanarayanan, M. Noel, A comparative evaluation on the voltammetric behavior of boron-doped diamond (BDD) and glassy carbon (GC) electrodes in different electrolyte media, *J. Electroanal. Chem.* 642 (1) (2010) 69–74, <https://doi.org/10.1016/j.jelechem.2010.02.007>.
- [14] J. Zhang, X. Yu, Z.-yan. Zhao, Z.-qiang. Zhang, J.-xuan. Pei, Z. Zhang, G.-ying. Cui, Adjusting surface morphology of substrate to improve the capacitive performance for the formed boron-doped diamond electrode, *Appl. Surf. Sci.* 491 (2019) 814–822, <https://doi.org/10.1016/j.apusc.2019.05.105>.
- [15] H. Fu, H. Zhuang, L. Yang, T. Hantschel, S. Ma, Z. Zhang, X. Jiang, Synthesis and characterization of boron doped diamond/ β -SiC composite films, *Appl. Phys. Lett.* 110 (2017) 031601(1)–031601(5), <https://doi.org/10.1063/1.4974295>.
- [16] G.V. Kornienko, N.V. Chaenko, N.G. Maksimov, V.L. Kornienko, V.P. Varnin, Electrochemical oxidation of phenol on boron-doped diamond electrode, *Russ. J. Electrochem.* 47 (2) (2011) 225–229, <https://doi.org/10.1134/S102319351102011X>.
- [17] M.A. Rodrigo, P.A. Michaud, I. Duo, M. Panizza, G. Cerisola, C. Cominellis, Oxidation of 4-chlorophenol at boron-doped diamond electrode for wastewater treatment, *J. Electrochem. Soc.* 148 (2001) D60–D64, <https://doi.org/10.1149/1.1362545>.
- [18] F. Montilla, P.A. Michaud, E. Morallón, J.L. Vázquez, C. Cominellis, Electrochemical oxidation of benzoic acid at boron-doped diamond electrodes, *Electrochim. Acta* 47 (21) (2002) 3509–3513, [https://doi.org/10.1016/S0013-4686\(02\)00318-3](https://doi.org/10.1016/S0013-4686(02)00318-3).
- [19] E. Brillas, I. Sirés, C. Arias, P.Lluís. Cabot, F. Centellas, R.María. Rodríguez, José.A. Garrido, Mineralization of paracetamol in aqueous medium by anodic oxidation with a boron-doped diamond electrode, *Chemosphere* 58 (4) (2005) 399–406, <https://doi.org/10.1016/j.chemosphere.2004.09.028>.
- [20] G. Loos, T. Scheers, K. Van Eyck, A. Van Schepdael, E. Adams, B. Van der Bruggen, D. Cabooter, R. Dewil, Electrochemical oxidation of key pharmaceuticals using a boron doped diamond electrode, *Sep. Purif. Technol.* 195 (2018) 184–191, <https://doi.org/10.1016/j.seppur.2017.12.009>.
- [21] L. Micheletti, B. Coldibeli, C.A.R. Salamanca-Neto, L.C. Almeida, E.R. Sartori, Assessment of the use of boron-doped diamond electrode for highly sensitive voltammetric determination of the azo-dye carmoisine E–122 in food and environmental matrices, *Talanta* 220 (2020) 121417–121423, <https://doi.org/10.1016/j.talanta.2020.121417>.
- [22] C. Candia-Onfray, N. Espinoza, E.B. Sabino da Silva, C. Toledo-Neira, L.C. Espinoza, R. Santander, V. García, R. Salazar, Treatment of winery wastewater by anodic oxidation using BDD electrode, *Chemosphere* 206 (2018) 709–717, <https://doi.org/10.1016/j.chemosphere.2018.04.175>.
- [23] İ. Özbay, N. Polat, Electro-oxidation of woodworking wastewater by using boron-doped diamond electrode, *Int. J. Environ. Anal. Chem.* (2020), <https://doi.org/10.1080/03067319.2020.1836173>.
- [24] X. Li, H. Li, M. Li, C. Li, D. Sun, Y. Lei, B. Yang, Preparation of a porous boron-doped diamond/Ta electrode for the electrocatalytic degradation of organic pollutants, *Carbon* 129 (2018) 543–551, <https://doi.org/10.1016/j.carbon.2017.12.052>.
- [25] N. Klidi, D. Clematis, M. Delucchi, A. Gadri, S. Ammar, M. Panizza, Applicability of electrochemical methods to paper mill wastewater for reuse. Anodic oxidation with BDD and TiRuSnO₂ anodes, *J. Electroanal. Chem.* 815 (2018) 16–23, <https://doi.org/10.1016/j.jelechem.2018.02.063>.
- [26] M. Cardoso, Éder.D. de Oliveira, M.L. Passos, Chemical composition and physical properties of black liquors and their effects on liquor recovery operation in Brazilian pulp mills, *Fuel* 88 (4) (2009) 756–763, <https://doi.org/10.1016/j.fuel.2008.10.016>.
- [27] M. Haddad, R. Labrecque, L. Bazinet, O. Savadogo, J. Paris, Effect of process variables on the performance of electrochemical acidification of Kraft black liquor by electro-dialysis with bipolar membrane, *Chem. Eng. J.* 304 (2016) 977–985, <https://doi.org/10.1016/j.cej.2016.07.030>.
- [28] A.P. Marques, D.V. Evtuguin, S. Magina, F.M.L. Amado, A. Prates, Chemical composition of Spent liquors from acidic magnesium-based Sulphite pulping of Eucalyptus globulus, *J. Wood Chem. Technol.* 29 (4) (2009) 322–336, <https://doi.org/10.1080/027738110903207754>.
- [29] R.C.P. Oliveira, M. Mateus, D.M.F. Santos, Chronoamperometric and chronopotentiometric investigation of Kraft black liquor, *Int. J. Hydrogen Energy* 43 (35) (2018) 16817–16823, <https://doi.org/10.1016/j.ijhydene.2018.01.046>.
- [30] W. Zhu, H. Theliander, Precipitation of lignin from softwood black liquor: An investigation of the equilibrium and molecular properties of lignin, *BioResources* 10 (2015) 1696–1714, <https://doi.org/10.15376/biores.10.1.1696-1715>.
- [31] L. Kouisni, A. Gagné, K. Maki, P. Holt-Hindle, M. Paleologou, LignoForce system for the recovery of lignin from black liquor: feedstock options, odor profile, and product characterization, *ACS Sustain. Chem. Eng.* 4 (2016) 5152–5159, <https://doi.org/10.1021/acssuschemeng.6b00907>.
- [32] L. Kouisni, P. Holt-Hindle, K. Maki, M. Paleologou, The LignoForce System™: A new process for the production of high-quality lignin from black liquor, *J-FOR* 2 (2012) 6–10.
- [33] P. Tomani, The lignoboost process, *Cellul. Chem. Technol.* 44 (2010) 53–58.
- [34] A.-S. Jönsson, A.-K. Nordin, O. Wallberg, Concentration and purification of lignin in hardwood kraft pulping liquor by ultrafiltration and nanofiltration, *Chem. Eng. Res. Des.* 86 (11) (2008) 1271–1280, <https://doi.org/10.1016/j.cherd.2008.06.003>.
- [35] W. Jin, R. Tolba, J. Wen, K. Li, A. Chen, Efficient extraction of lignin from black liquor via a novel membrane-assisted electrochemical approach, *Electrochim. Acta* 107 (2013) 611–618, <https://doi.org/10.1016/j.electacta.2013.06.031>.
- [36] C.A.E. Costa, P.C.R. Pinto, Alfrío.E. Rodrigues, Lignin fractionation from E. Globulus kraft liquor by ultrafiltration in a three stage membrane sequence, *Sep. Purif. Technol.* 192 (2018) 140–151, <https://doi.org/10.1016/j.seppur.2017.09.066>.
- [37] R. Paliwal, S. Uniyal, M. Verma, A. Kumar, J.P.N. Rai, Process optimization for biodegradation of black liquor by immobilized novel bacterial consortium, *Desalin. Water Treat.* 57 (40) (2016) 18915–18926, <https://doi.org/10.1080/19443994.2015.1092892>.
- [38] R.C.P. Oliveira, M.M. Mateus, D.M.F. Santos, On the oxidation of kraft black liquor for lignin recovery: a voltammetric study, *J. Electrochem. Soc.* 166 (2019) E547–E553, <https://doi.org/10.1149/2.0131916jes>.
- [39] H. ROYGHATAK, Electrolysis of black liquor for hydrogen production: Some initial findings, *Int. J. Hydrogen Energy* 31 (7) (2006) 934–938, <https://doi.org/10.1016/j.ijhydene.2005.07.013>.
- [40] H.R. Ghatak, S. Kumar, P.P. Kundu, Electrode processes in black liquor electrolysis and their significance for hydrogen production, *Int. J. Hydrogen Energy* 33 (12) (2008) 2904–2911, <https://doi.org/10.1016/j.ijhydene.2008.03.051>.
- [41] M. Haddad, S. Mikhaylin, L. Bazinet, O. Savadogo, J. Paris, Electrochemical acidification of kraft black liquor: effect of fouling and chemical cleaning on ion exchange membrane integrity, *ACS Sustain. Chem. Eng.* 5 (2017) 168–178, <https://doi.org/10.1021/acssuschemeng.6b01179>.
- [42] J.-N. Cloutier, O. Savadogo, J. Paris, M. Perrier, R. Labrecque, N. Kandeve, P. Champagne, Effect of the basic electrochemical cell operating parameters on the performance of the electrolysis of kraft pulping black liquor, *ECS Trans.* 80 (10) (2017) 871–891, <https://doi.org/10.1149/08010.0871ecst>.
- [43] G. Nong, Z. Zhou, S. Wang, Generation of hydrogen, lignin and sodium hydroxide from pulping black liquor by electrolysis, *Energies* 9 (2016) 13–23, <https://doi.org/10.3390/en9010013>.
- [44] M. Zaied, N. Bellakhal, Electrocoagulation treatment of black liquor from paper industry, *J. Hazard. Mater.* 163 (2–3) (2009) 995–1000, <https://doi.org/10.1016/j.jhazmat.2008.07.115>.
- [45] S. Garcia-Segura, J.D. Ocon, M.N. Chong, Electrochemical oxidation remediation of real wastewater effluents - A review, *Process Saf. Environ. Prot.* 113 (2018) 48–67, <https://doi.org/10.1016/j.psep.2017.09.014>.
- [46] P. Parpot, A.P. Bettencourt, A.M. Carvalho, E.M. Belgsir, Biomass conversion: Attempted electrooxidation of lignin for vanillin production, *J. Appl. Electrochem.* 30 (2000) 727–731, <https://doi.org/10.1023/A:1004003613883>.

- [47] H.L. Chum, D.W. Sopher, H.A. Schroeder, Electrochemistry of lignin materials and derived compounds, *Fundam. Thermochem. Biomass Convers.* (1985) 1103–1113, https://doi.org/10.1007/978-94-009-4932-4_62.
- [48] E.I. Kovalenko, O.V. Popova, A.A. Aleksandrov, T.G. Galikyan, Electrochemical modification of lignins, *Russ. J. Electrochem.* 36 (7) (2000) 706–711, <https://doi.org/10.1007/BF02757667>.
- [49] O. Movil-Cabrera, A. Rodriguez-Silva, C. Arroyo-Torres, J.A. Staser, Electrochemical conversion of lignin to useful chemicals, *Biomass and Bioenergy* 88 (2016) 89–96, <https://doi.org/10.1016/j.biombioe.2016.03.014>.
- [50] H. Zhu, Y. Chen, T. Qin, L. Wang, Y. Tang, Y. Sun, P. Wan, Lignin depolymerization via an integrated approach of anode oxidation and electro-generated H₂O₂ oxidation, *RSC Adv.* 4 (2014) 6232–6238, <https://doi.org/10.1039/c3ra47516f>.
- [51] A. Caravaca, W.E. Garcia-Lorefece, S. Gil, A. de Lucas-Consuegra, P. Vernoux, Towards a sustainable technology for H₂ production: Direct lignin electrolysis in a continuous-flow polymer electrolyte membrane reactor, *Electrochem. Commun.* 100 (2019) 43–47, <https://doi.org/10.1016/j.elecom.2019.01.016>.
- [52] D. Schmitt, C. Regenbrecht, M. Hartmer, F. Stecker, S.R. Waldvogel, Highly selective generation of vanillin by anodic degradation of lignin: A combined approach of electrochemistry and product isolation by adsorption, *Beilstein J. Org. Chem.* 11 (2015) 473–480, <https://doi.org/10.3762/bjoc.11.53>.
- [53] S. Stiefel, J. Lölsberg, L. Kipschagen, R. Möller-Gulland, M. Wessling, Controlled depolymerization of lignin in an electrochemical membrane reactor, *Electrochem. Commun.* 61 (2015) 49–52, <https://doi.org/10.1016/j.elecom.2015.09.028>.
- [54] K. Pan, M. Tian, Z.H. Jiang, B. Kjartanson, A. Chen, Electrochemical oxidation of lignin at lead dioxide nanoparticles photoelectrodeposited on TiO₂ nanotube arrays, *Electrochim. Acta* 60 (2012) 147–153, <https://doi.org/10.1016/j.electacta.2011.11.025>.
- [55] M. Tsigkourakos, T. Hantschel, S.D. Janssens, K. Haenen, W. Vandervorst, Spin-seeding approach for diamond growth on large area silicon-wafer substrates, *Phys. Status Solidi Appl. Mater. Sci.* 209 (9) (2012) 1659–1663, <https://doi.org/10.1002/pssa.201200137>.
- [56] J.G. Buijnsters, M. Tsigkourakos, T. Hantschel, F.O.V. Gomes, T. Nuytten, P. Favia, H. Bender, K. Arstila, J.-P. Celis, W. Vandervorst, Effect of boron doping on the wear behavior of the growth and nucleation surfaces of micro- and nanocrystalline diamond films, *ACS Appl. Mater. Interfaces* 8 (39) (2016) 26381–26391, <https://doi.org/10.1021/acsami.6b08083>.
- [57] André.F. Sartori, S. Orlando, A. Bellucci, D.M. Trucchi, S. Abrahami, T. Boehme, T. Hantschel, W. Vandervorst, J.G. Buijnsters, Laser-induced periodic surface structures (LIPSS) on heavily boron-doped diamond for electrode applications, *ACS Appl. Mater. Interfaces* 10 (49) (2018) 43236–43251, <https://doi.org/10.1021/acsami.8b15951>.
- [58] ASTM E1755-01 (2020), Standard test method for ash in biomass, ASTM International, West Conshohocken, PA, USA, 2020. 10.1520/E1755-01R07.2
- [59] ASTM D1217-15 (2015), Standard Test Method for Density and Relative Density (Specific Gravity) of Liquids by Bingham Pycnometer, ASTM International, West Conshohocken, PA, USA, 2015. 10.1520/D1217-15
- [60] Acid-insoluble lignin in wood and pulp (T 222 om-02, revised), Tappi Standards, Tappi, Peachtree Corners, GA, USA, 2006
- [61] A. Merlen, J.G. Buijnsters, C. Pardanaud, A guide to and review of the use of multiwavelength Raman spectroscopy for characterizing defective aromatic carbon solids: From graphene to amorphous carbons, *Coatings* 7 (2017) 153–208. 10.3390/coatings7100153
- [62] M.T. Andreuccetti, B.S. Leite, J.V.H. D'Angelo, Eucalyptus black liquor - Density, viscosity, solids and sodium sulfate contents revisited, *O Papel* 72 (2011) 52–57.
- [63] Robisnéa.A. Ribeiro, S.V. Júnior, H. Jameel, H.-M. Chang, R. Narron, X. Jiang, J.L. Colodette, Chemical study of kraft lignin during alkaline delignification of *E. urophylla* x *E. grandis* hybrid in low and high residual effective alkali, *ACS Sustain. Chem. Eng.* 7 (12) (2019) 10274–10282, <https://doi.org/10.1021/acsschemeng.8b06635>.
- [64] W. Zhu, H. Theliander, Equilibrium of lignin precipitation, in: *Proceedings of the 16th ISWFPC*, 2011, pp. 195–199.
- [65] W. Zhu, G. Westman, H. Theliander, Investigation and characterization of lignin precipitation in the lignoboost process, *J. Wood Chem. Technol.* 34 (2) (2014) 77–97, <https://doi.org/10.1080/02773813.2013.838267>.
- [66] A. Dieste, L. Clavijo, A.I. Torres, S. Barbe, I. Oyarbide, L. Bruno, F. Cassella, Lignin from Eucalyptus spp. kraft black liquor as biofuel, *Energy and Fuels* 30 (12) (2016) 10494–10498, <https://doi.org/10.1021/acs.energyfuels.6b02086>.
- [67] J. Fatehi, P. Chen, Extraction of technical lignins from pulping spent liquors, challenges and opportunities, In: *Production of biofuels and chemicals from lignin. Biofuels and biorefineries* (2016). Springer, Singapore. 10.1007/978-981-10-1965-4_2
- [68] R. Alén, S. Rytönen, P. McKeough, Thermogravimetric behavior of black liquors and their organic constituents, *J. Anal. Appl. Pyrolysis* 31 (1995) 1–13, [https://doi.org/10.1016/0165-2370\(94\)00811-E](https://doi.org/10.1016/0165-2370(94)00811-E).
- [69] G. Socrates, Infrared and Raman characteristic group frequencies. Tables and charts, 3rd Ed., John Wiley & Sons, Chichester, UK (2001). 10.1002/jrs.1238
- [70] P.J. Larkin, IR and Raman Spectroscopy, 1st Ed., Elsevier, Waltham, MA, USA, 2011. 10.1017/CBO9781107415324.004
- [71] J. Coates, Interpretation of infrared spectra, a practical approach, in: *Encyclopedia of Analytical Chemistry* 10815–10837, John Wiley & Sons Ltd, Chichester 2000. 10.1002/9780470027318.a5606
- [72] T. Maisarah, A. Zuraida, A. Marjan, The effect of black liquor on rattan waste binderless board (BPB) produced via digestion-hot pressing (DHP) process, *ARPN J. Eng. Appl. Sci.* 10 (2015) 9753–9758.
- [73] D.F. Leclerc, Fourier transform infrared spectroscopy in the pulp and paper industry, in: *Encyclopedia of Analytical Chemistry* 8361–8388, John Wiley & Sons Ltd, Chichester 2000. <https://doi.org/10.1002/9780470027318.a2203>
- [74] J. Rodrigues, O. Faix, H. Pereira, Determination of lignin content of Eucalyptus globulus wood using FTIR spectroscopy, *Holzforschung* 52 (1) (1998) 46–50, <https://doi.org/10.1515/hfsg.1998.52.1.46>.
- [75] A.S. Jääskeläinen, M. Nuopponen, P. Axelsson, M. Halttunen, M. Löijä, T. Vuorinen, Determination of lignin distribution in pulps by FTIR ATR spectroscopy, *J. Pulp Pap. Sci.* 29 (2003) 328–331.
- [76] A. Bermello, M.D. Valle, U. Orea, L.R. Carballo, Characterization by infrared spectrometry of lignins of three Eucalyptus species, *Int. J. Polym. Mater.* 51 (6) (2002) 557–566, <https://doi.org/10.1080/00914030209696301>.
- [77] L. Czuchajowski, S. Duraj, M. Kucharska, Vibrational Studies of Na₂SO₄, K₂SO₄, NaHSO₄ and KHSO₄ crystals, *Rasayan J. Chem.* 2 (2009) 981–989, [https://doi.org/10.1016/0022-2860\(76\)82004-2](https://doi.org/10.1016/0022-2860(76)82004-2).
- [78] R.C.P. Oliveira, M. Mateus, D.M.F. Santos, Black liquor electrolysis for hydrogen and lignin extraction, *ECS Trans.* 72 (22) (2016) 43–53, <https://doi.org/10.1149/07222.0043ecst>.
- [79] E.M. Espinoza, J.A. Clark, J. Soliman, J.B. Derr, M. Morales, V.I. Vullev, Practical aspects of cyclic voltammetry: how to estimate reduction potentials when irreversibility prevails, *J. Electrochem. Soc.* 166 (2019) H3175–H3187, <https://doi.org/10.1149/2.0241905jes>.
- [80] N. Aristov, A. Habekost, Cyclic voltammetry - a versatile electrochemical method investigating electron transfer processes, *World, J. Chem. Educ.* 3 (2015) 115–119, <https://doi.org/10.12691/wjce-3-5-2>.
- [81] R.G. Compton, E. Laborda, K.R. Ward, Understanding voltammetry: simulation of electrode processes, 1st Ed., Imperial College Press, Oxford, UK, 2014. 10.1142/P910
- [82] A.J. Bard, L.R. Faulkner, *Electrochemical Methods: Fundamentals and Applications*, 2nd Ed., John Wiley & Sons, Inc., 2001. 10.1016/B978-0-08-098353-0.00003-8
- [83] C.M.A. Brett, A.M.O. Brett, *Electrochemistry: Principles, Methods, and Applications*, 1st Ed., Oxford University Press Inc., Oxford, UK, 1993.
- [84] P.C. Pinto, D.V. Evtuguin, C. Pascoal Neto, A.J.D. Silvestre, Behavior of Eucalyptus globulus lignin during kraft pulping. I. Analysis by chemical degradation methods, *J. Wood Chem. Technol.* 22 (2-3) (2002) 93–108, <https://doi.org/10.1081/WCT-120013355>.
- [85] P.C. Pinto, D.V. Evtuguin, C.P. Neto, A.J.D. Silvestre, F.M.L. Amado, Behavior of Eucalyptus globulus lignin during kraft pulping. II. Analysis by NMR, ESI/MS, and GPC, *J. Wood Chem. Technol.* 22 (2-3) (2002) 109–125, <https://doi.org/10.1081/WCT-120013356>.
- [86] Inês.C. Belo, R.C.P. Oliveira, M. Mateus, João.C.M. Bordado, P. Pinto, D.M.F. Santos, Development of a black liquor electrolyzer for lignin extraction, *ECS Trans.* 86 (4) (2018) 3–9, <https://doi.org/10.1149/08604.0003ecst>.
- [87] M. Leschinsky, G. Zuckerstätter, H.K. Weber, R. Patt, H. Sixta, Effect of autohydrolysis of Eucalyptus globulus wood on lignin structure. Part 1: Comparison of different lignin fractions formed during water prehydrolysis, *Holzforschung* 62 (2008) 645–652, <https://doi.org/10.1515/HF.2008.117>.
- [88] M. Leschinsky, G. Zuckerstätter, H.K. Weber, R. Patt, H. Sixta, Effect of autohydrolysis of Eucalyptus globulus wood on lignin structure. Part 2: Influence of autohydrolysis intensity, *Holzforschung* 62 (2008) 653–658, <https://doi.org/10.1515/HF.2008.133>.
- [89] D.V. Evtuguin, C.P. Neto, A.M.S. Silva, P.M. Domingues, F.M.L. Amado, D. Robert, O. Faix, Comprehensive study on the chemical structure of dioxane lignin from plantation Eucalyptus globulus wood, *J. Agric. Food Chem.* 49 (9) (2001) 4252–4261, <https://doi.org/10.1021/jf010315d>.